Journal of The Electrochemical Society, **156** (4) P68-P73 (2009)
0013-4651/2009/156(4)/P68/6/$23.00 © The Electrochemical Society

Preparation of Microfiber and Smooth Film Conducting Polymer Electrodes

Anthony D. Kammerich, Yasmin Srivastava, Kristen N. Hargett, Victoria S. R. Harrison, and Judith F. Rubinson*[,z]

Department of Chemistry, Georgetown University, Washington, DC 20057, USA

As part of a long-range effort involving the design and fabrication of electrodes for in vivo use, we describe herein a method for the production of conducting polymer fibers with diameters on the order of a few micrometers. This method has been shown to be applicable to several different combinations of monomers [pyrrole, *N*-methylpyrrole, 3-methylthiophene, poly(3,4-ethylene dioxythiophene)], deposition substrates (Pt, stainless steel), and dopant ions (dodecyl benzene sulfonate, perchlorate, chloride, polymethylmethacrylate). Cyclic voltammetric characterization shows that the background current is minimal, and normal behavior is seen for the ferri/ferrocyanide couple with the exception of a slightly increased peak separation. An ancillary benefit of these studies is the production of extremely smooth films of these polymers, even in cases where the films are up to 20 μm thick.
© 2009 The Electrochemical Society. [DOI: 10.1149/1.3078153] All rights reserved.

Manuscript submitted October 23, 2008; revised manuscript received December 24, 2008. Published February 13, 2009.

Over the past 30 years, conducting polymers have shown potential for applications in a wide variety of areas, ranging from photovoltaic design to electrocatalysis to sensors to biomaterials. An important factor in their success has been the advances in synthetic methods for these polymers and tailoring of their morphology on both the molecular and macroscopic scale.[1]

Over the same period, there has been a growing need for electrodes with diameters on the order of a micrometer. This scale insures that the electrodes are large enough that manipulation is facile, the electrode is physically rugged, the resistance is low, and the resulting currents during electroanalytical measurements are sufficiently large to measure with commercially available instruments. At the same time, production of electrodes on this scale and slightly below have implications for applications such as scanning electrochemical microscopy (micrometer to submicrometer resolution), microelectronics, and design of electrodes for in vivo use (minimization of trauma to the area to be investigated).

Recently, Michael et al. have reported that when in vivo studies of neurotransmitter release are carried out using electrodes with diameters even as small as 10 μm, there is sufficient damage to brain tissue that the results are distorted.[2] When the electrode diameter is further reduced to 1 μm, such damage is decreased and it becomes possible to monitor the level of neurotransmitters released from single sites on a neuron.[3] Thus, successful fabrication of electrodes with small diameters would constitute a significant advance in carrying out such studies. These ultramicroelectrodes would also be useful for biomedical applications such as in vivo analysis and sensing.[4,5] When the electrodes are fibers of conducting polymers, there is the additional advantage of a more biologically benign surface[4,6,7] for long-term implanted biomedical devices such as those used for deep-brain-stimulation electrodes in the treatment of Parkinson's disease[8] or epilepsy.[9]

There are a number of methods that have been reported in the literature for production of nano- or microscale conducting polymer fibers from heteroarylenes. These include electrodeposition from a monomer/dopant solution onto or in a template[10] or microchannel,[11] wet spinning from a spinnerette containing an aqueous polymer/dopant solution into acetone,[12] electrochemical production from micelles containing monomer solutions,[13] production of fibers at the interface of an aqueous/organic biphasic system,[14] self-assembly,[13,15] electrodeposition from solution onto the tip of a larger electrode,[16-18] or dry electrospinning across an air gap through a kilovolt potential.[19] It is possible to vary the heteroarylene monomer to produce polymers with different heteroatoms and different chains of atoms attached on the side of the ring opposite the heteroatom.

There are, however, difficulties with regard to connection to a macroscopic contact which impact the routine use of these fibers as electrodes. The fabrication procedure described here is an extension of the procedure reported by Li and White[20] involving electrodeposition of polymer from a monomer solution onto the tip of a much larger diameter wire. This enables easier connection to a device for monitoring of current or potential. This earlier procedure resulted in the production of polythiophene fiber electrodes under rapid-flow conditions of monomer solution past the tip of a 127 μm Pt electrode.[16] The studies show that by varying the other components in solution, the flow rate of the solution and the dimensions and shape of the tube between the electrodes, they can vary the shape and diameter of the fiber that grows from the tip of the working electrode.[16,19] A modified form of this apparatus has been used in our laboratory to produce ultramicroelectrodes based on several different monomers, including pyrrole, *N*-methylpyrrole, 3-methylthiophene, and poly(3,4-ethylenedioxythiophene). The working (substrate) electrodes have included Pt, stainless steel, and gold, while dopant ions have included dodecylbenzene sulfonate, perchlorate, chloride, tetrafluoroborate, and polymethylmethacrylate.

Experimental

Chemicals.— Platinum and gold wires were obtained from Alfa Aesar and were (except for 25 μm wire) 99.9998% purity. The 25 μm wire was 99.95% purity. Stainless steel wire was also obtained from Alfa Aesar. Acetonitrile was purchased from Fisher Scientific, and the 18.2 MΩ water used for aqueous deposition experi-

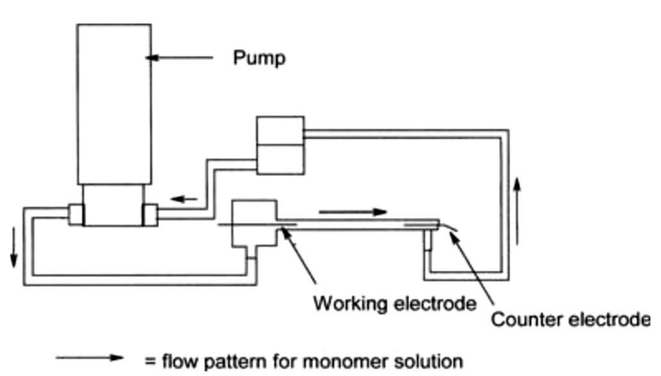

Figure 1. Schematic of flow-cell setup.

* Electrochemical Society Active Member.
z E-mail: jfr@georgetown.edu

Downloaded on 2016-09-15 to IP 130.203.136.75 address. Redistribution subject to ECS terms of use (see ecsdl.org/site/terms_use) unless CC License in place (see abstract).

Table II. Optimum polymerization parameters for the formation of a poly-*N*-methylpyrrole fiber.

Reaction zone diameter	2 mm
Working electrode	0.1 mm Pt
Auxiliary electrode	0.5 mm Pt
Deposition solution	aqueous 0.1 M methylpyrrole +0.1 M NaDBS
Flow rate	100 mL/min
Electrode separation	3.5–4.0 cm
Deposition potential	1.3 V
Deposition time	15 min

ments was produced using a Waters RiOs 5 reverse osmosis system. All chemicals were reagent grade and used without further purification.

Deposition apparatus.— A deposition cell was fabricated in-house, which allowed for facile variation of the parameters that affected the shape, diameter, and length of the fiber (or fibers) produced. A model QV2 FMI fluid-transfer pump was used to continuously recirculate monomer solution through the cell (Fig. 1).

For production of fibers, the working and counter electrodes were sealed in a glass capillary for insertion into the screw connection seals at each end of the apparatus. The electrodes were rinsed thoroughly with water or acetonitrile in an ultrasonic bath to remove any surface dirt and oils before use. Potential was applied using an IBM model 225, Radiometer Voltalab 10, or Radiometer Voltalab 80 potentiostat in a two-electrode configuration, and current was monitored throughout the deposition.

For the film depositions, both a flow cell and a standard cell were used. The working electrodes were manufactured by soldering platinum to copper and sealing the connections inside of a glass pipette with Varian Torr Seal, so that only the platinum was exposed to the solution. The portion of the platinum that would come into contact with the solder was coated with copper before the soldering process to prevent degradation of the connection.[21] The auxiliary electrode was a 500 μm platinum wire which was inserted through a septum. The substrate electrodes for film deposition were cleaned by sonicating in a series of solutions (NaOH, H_2SO_4, hexane, and ethanol) before deposition. Potential was controlled using a Radiometer Voltalab 80 potentiostat.

Optimization of Deposition Parameters

To determine the effect of deposition parameters on film and fiber formation, parameters were varied for polypyrrole fiber production, and their values are summarized in Table I. Parameters which were held constant were monomer concentration (0.1 M) and diameter of counter electrode (0.5 mm). The films were deposited in a standard cell by cyclic voltammetry (CV) cycling between 0 and 1800 mV. The optimum parameters were determined and are summarized in Table II. The success with the formation of polypyrrole led to the study being expanded to *N*-methylpyrrole to decrease the likelihood of α, β linkage, known to lead to degradation.[22]

Flow rate.— The volume flow rate and the diameter of the reaction region both impact the linear flow rate past the tip of the deposition electrode. At high flow rates, there was production of

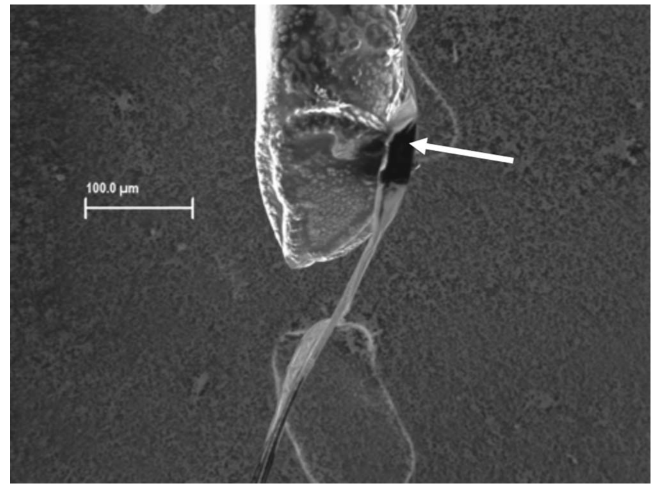

Figure 2. Poly-*N*-methylpyrrole fiber grown from the tip of a 100 μm Pt electrode at high flow rates.

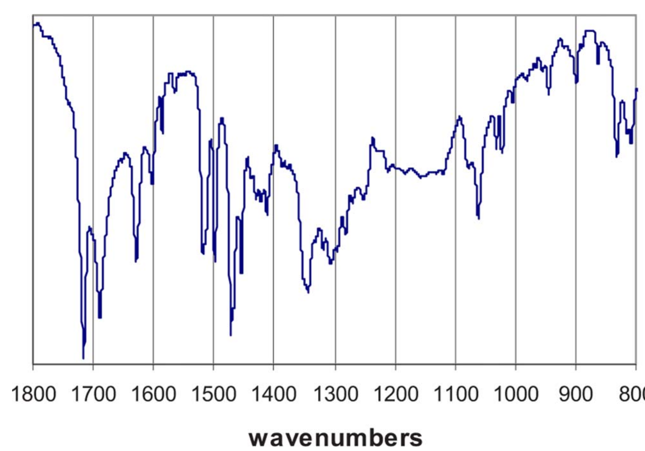

Figure 3. (Color online) FTIR of poly-*N*-methylpyrrole.

Table I. Variation of deposition parameters for poly-*N*-methylpyrrole deposition.

Variation of…,	Working electrode diameter (μm)	Flow rate (mL/min)	Dopant (M)	Electrode separation (cm)	Deposition potential (V)	Diameter of reaction region (mm)
Flow rate	100	35–120	0.1	3.5	1.3	3
Diameter of reaction region	100	60	0.1	3.5	1.3	2–3
Anode Diameter	25–250	60	0.1	3.5	1.3	3
[Dopant]	100	60	0.05–0.2	3.5	1.3	3
Electrode separation	100	60	0.1	0.3–7.0	1.3	3
Deposition potential	100	60	0.1	3.5	0.8–1.3	3

Downloaded on 2016-09-15 to IP 130.203.136.75 address. Redistribution subject to ECS terms of use (see ecsdl.org/site/terms_use) unless CC License in place (see abstract).

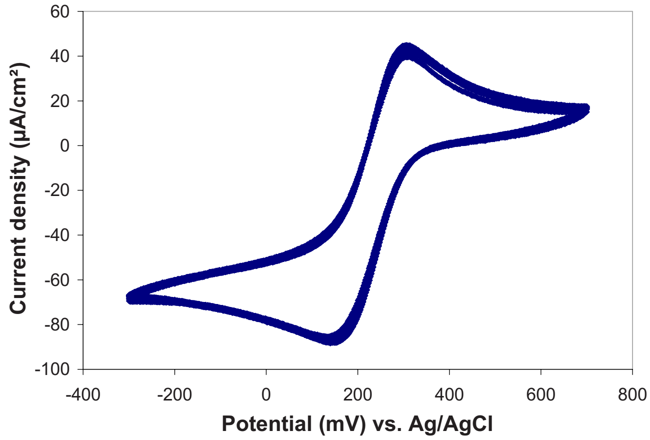

Figure 4. (Color online) CV of 50 mM ferricyanide in 0.1 M KCl at poly-*N*-methylpyrrole electrode.

multiple-ribbon-like fibers not only at the tip but also along the sides of the electrode (Fig. 2). However, at lower flow rates there were fewer fibers, and these tended to extend out from the deposition electrode in the direction of flow. The linear flow rate appears to be the most important factor in terms of aspect ratio, because for a given volume flow, the fiber diameter decreased significantly as the reaction region diameter decreased. In order to determine the linearity of the flow of the solution past the end of the electrode, the Reynolds number was calculated. It was found to be approximately 2100, which falls in the region between laminar flow and turbulent flow.

Electrode diameter and interelectrode separation.— As might be expected from the variations produced in current density and electric field, the diameter of the deposition electrode and its distance from the counter electrode also affected the relative probability that a single fiber would be produced vs a large number of fibers forming at the tip or on the sides. Decreasing the tip diameter resulted in a significant decrease in the diameter of the fiber produced under the same flow and concentration conditions. Cutting the end of the electrodes at an angle to produce a high aspect ratio at the tip further increased the likelihood of producing a single fiber off the end. The separation between the electrodes had a major impact on the aspect

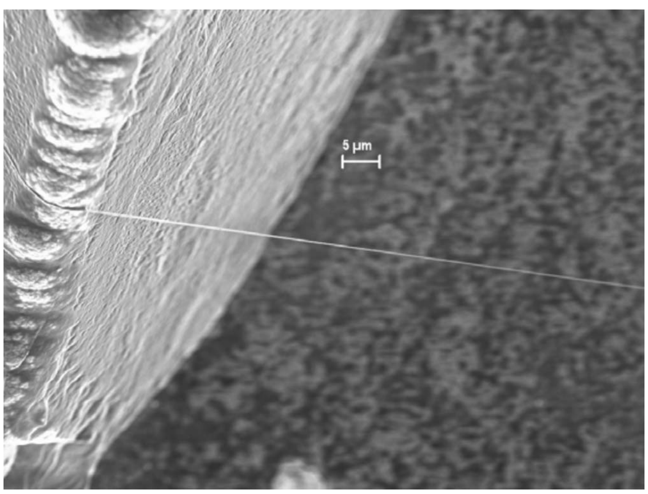

Figure 5. Poly-*N*-methylpyrrole fiber produced using ideal conditions reported in Table II.

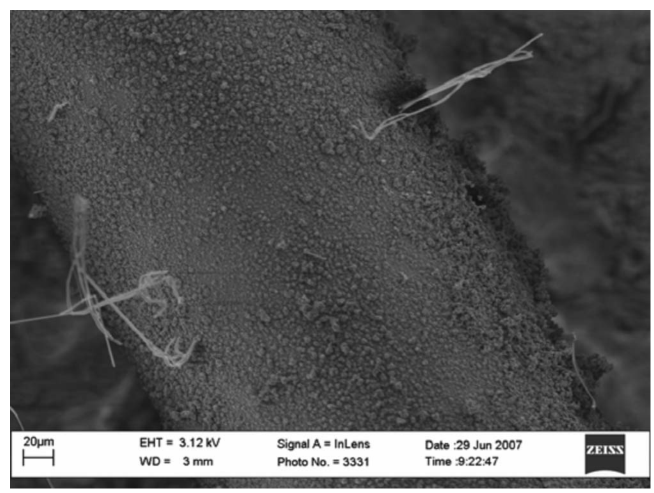

Figure 7. SEM of P3MT on Pt.

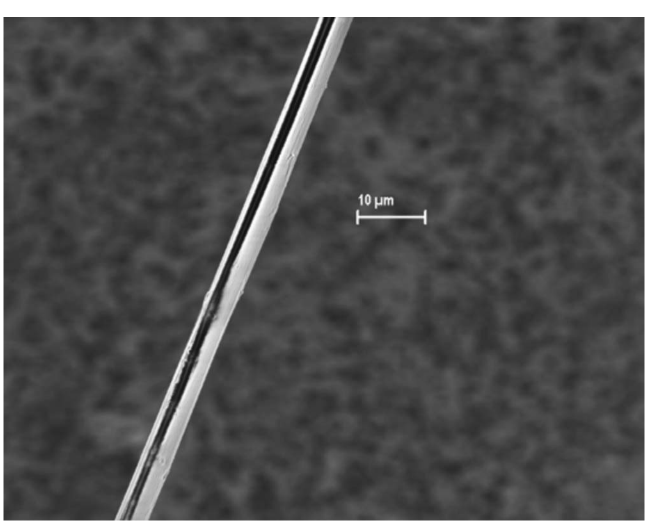

Figure 6. Poly-*N*-methylpyrrole fiber produced over a longer period of time using ideal conditions reported in Table II.

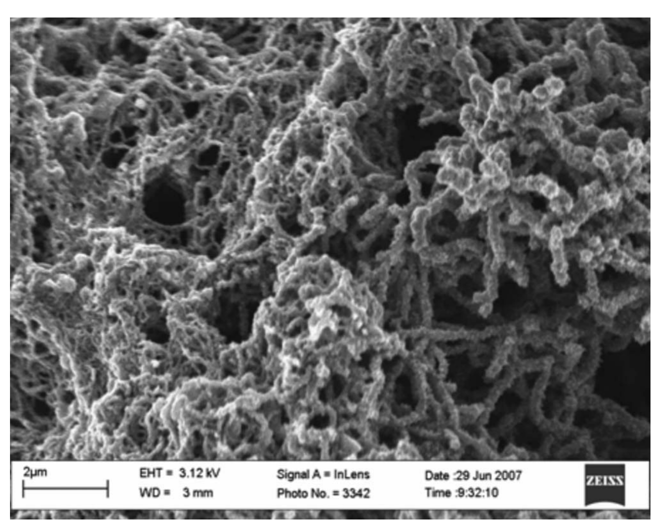

Figure 8. SEM of the P3MT thick film resulting from an extended growth time.

Downloaded on 2016-09-15 to IP 130.203.136.75 address. Redistribution subject to ECS terms of use (see ecsdl.org/site/terms_use) unless CC License in place (see abstract).

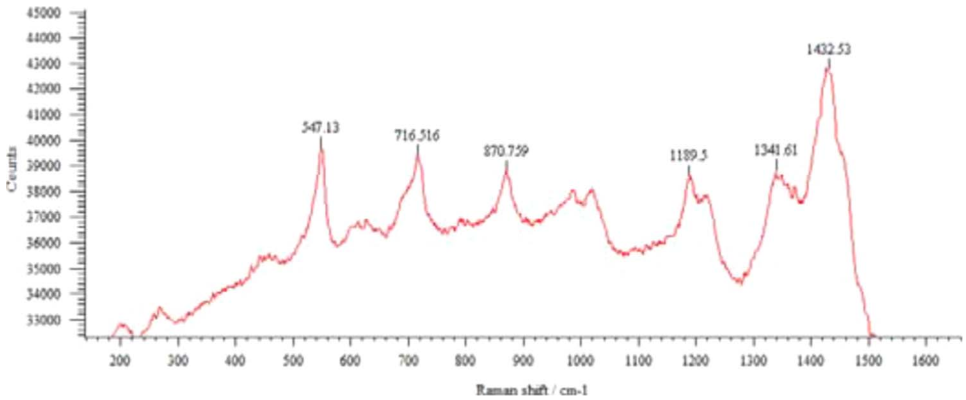

Figure 9. (Color online) P3MT Raman spectra.

ratio of the fibers produced. At the upper end of the range tested, longitudinal growth was slow. This meant that the diameter increased under these conditions.

Dopant concentration.— Background electrolyte concentrations that produced the highest-quality fibers (small uniform diameter, minimum number of fibers) occurred in the midrange of the values used. This range provided a trade-off between the rate of production, length of fibers, and the number of fibers produced. At low dopant concentrations (all other parameters remaining constant), the IR drop in the solution resulted in a slower deposition, and at the lowest concentrations, growth was not observed even after several hours. This consideration must be balanced with the relatively low solubility for some of the electrolytes.

Applied potential and deposition time.— Variation of the applied potential profoundly affects the kinetics of the deposition process. Potentials at the more positive end of the range tested resulted in rapid fiber growth from the tip. However, if the reaction is allowed to proceed at the same accelerated rate after the initial rapid formation of the fiber, polymer is deposited preferentially on the sides of the fiber (as opposed to the tip) and the diameter begins to increase. In addition, fibers begin to grow from nucleation sites on the sides of the electrode.

Deposition substrate.— The identity of the substrate electrode produces its greatest impact on the ruggedness of the interface between the deposition electrode and the fiber and on the time required for initiation of polymer formation. For example, fiber production from gold wires was extremely inefficient, with stainless steel being marginally more rugged and Pt being the most robust by far. For the pyrrole polymers this is consistent with prior results with film electrodes, but for the thiophene polymers this is surprising, as production of films on gold band and disk electrodes is widely reported.[23-26]

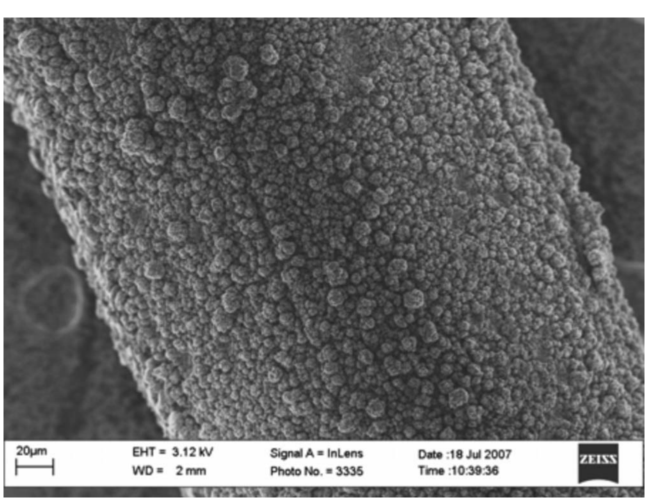

Figure 10. SEM of PEDOT on Pt.

Spectroscopic and electrochemical characterization.— Polypyrrole and poly-*N*-methylpyrrole fibers produced using the optimized parameters above were characterized by Fourier transform IR (FTIR) spectroscopy to confirm the identity of the fibers produced. The spectra exhibited the expected C–C single and double bond stretches at 1540 and 1488 cm^{-1}, respectively, as well as the 1036 cm^{-1} N–H bending mode[27] for polypyrrole (Fig. 3).

In order to assess the electrochemical utility of the electrodes, they were characterized using CV of ferri-/ferrocyanide. The behavior of the ferri-/ferrocyanide system on poly(*N*-methylpyrrole) fibers is shown in Fig. 4. The ΔE is slightly greater than that seen under ideal conditions, but the low background suggests that the electrodes are electrochemically useful. In addition, the current density–voltage dependence is not sigmoidal as would be expected. Both of these deviations from the expected behavior can be explained by slight retardation of electron-transfer kinetics at the polymer surface.[28]

High-Aspect-Ratio Poly-*N*-Methylpyrrole Fiber Production

Using the optimized conditions determined from the above studies and summarized in Table II, small fibers are seen to begin to form toward the end of the electrode, as seen in Fig. 5. The deposition time was then extended to approximately an hour, leading to production of a long fiber of poly-*N*-methylpyrrole that extended out from the tip of the working electrode (Fig. 2). The fiber had an overall length of 4.2 mm. The fiber consisted of a major fiber with a smaller ribbonlike structure wrapping around it for 550 μm down the fiber from the electrode, which extends away from the fiber and then terminates. Beyond this point, the main fiber is a uniform rod structure with a 5 μm diameter. It has no discernable surface features even when examined under high magnification (Fig. 6).

Results With Other Monomer/Substrate Combinations

With minor changes in flow rate and solution conditions and choice of appropriate oxidation potential, this fabrication process has been extended for use with 3-methylthiophene and aniline. Other dopants used have included dodecylbenzene sulfonate, chloride, perchlorate, tetrafluoroborate, and polymethylmethacrylate.

Raman microspectroscopic studies were carried out on a fiber produced from 3-methylthiophene/dodecylbenzenesulfonate solution, which contrasted the film on the surface of the platinum substrate with the fiber on its tip. The fiber showed a significant enhancement of fluorescence when excitation was carried out at 514.5 nm compared to film that is deposited on the sides of the anode. It is not clear at this time whether this is due to differences in conjugation length (and thus a shift of the absorption maximum to lower wavelengths and therefore differences in absorbance at this

Downloaded on 2016-09-15 to IP 130.203.136.75 address. Redistribution subject to ECS terms of use (see ecsdl.org/site/terms_use) unless CC License in place (see abstract).

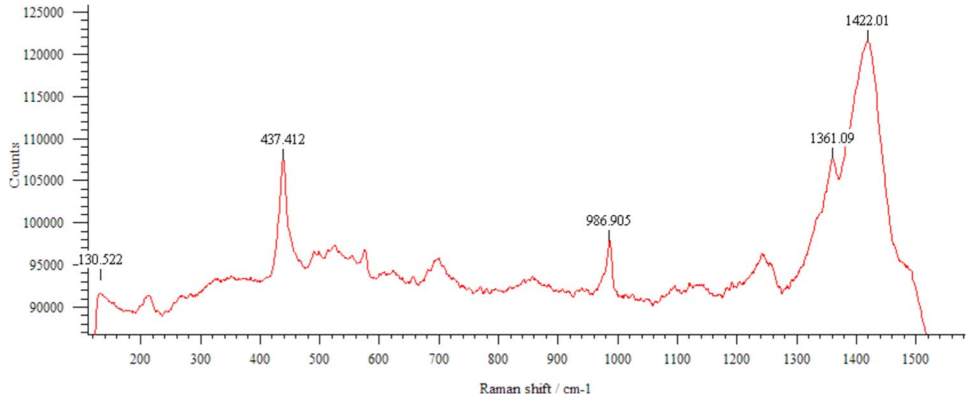

Figure 11. (Color online) PEDOT Raman spectra.

wavelength)[29] or to greater efficiency for the fluorescence process than that normally found for the polymer. This finding raises the possibility of analysis based on fluorescence quenching.

The effects of the identity of the dopant counterion lie primarily in the flexibility and the chemical stability of the polymer fiber produced, while the effect of the substrate electrode appeared in the durability of the substrate/fiber junction and in the rate of production of the fiber. For example, fibers produced at the platinum substrate grew to a few micrometers in length within 5 min and resulted in a robust interface at the electrode–fiber junction.

Films.— Based on the appearance of the films grown on the surface of the substrate wires, poly-3-methylthiophene (P3MT) and polyethylenedioxythiophene (PEDOT) also were prepared in a standard cell. A uniform P3MT coating appeared in a relatively short time period, under 5 min, with surface features about 1.5 μm in diameter with fibers growing off the sides of the electrodes (Fig. 7). These fibers, when examined under higher magnification, are smooth with no discernable features, much like those produced in the film-growth experiments. When the coating was allowed to grow for an extended period of time to a thickness of approximately 100 μm, the surface features grew into a spongelike material (Fig. 8). Raman spectroscopy obtained with excitation at 785 nm (Fig. 9) was employed to verify the identity and probe the doping levels in the films. The relative location of these peaks corresponds to those previously reported in literature.[30] The slight differences in intensities and positions can be attributed to a difference in the fractional doping in the sample.[31] The doping level of the film, y, can be calculated using the following equation[31]

$$0.087y - 2.279 = \ln\left(\frac{I_{ox}}{I_{red}}\right)$$

Based on the intensities at 1422 and 1480 wavenumbers (the peaks for the reduced and oxidized form, respectively), the doping level was calculated to be approximately 23%.

Thin films of PEDOT were also made and examined with the standard cell. The PEDOT films produced surface features similar in shape to those of the thin P3MT but larger (Fig. 10). The resulting features are about 5–10 μm in diameter. Raman spectra were also taken of the film (Fig. 11), and the major spectroscopic features again correspond to those previously reported.[32]

Conclusions

The procedure and apparatus described herein can be employed to produce robust fibers with diameters of 5–6 μm or less for 3-methylthiophene and *N*-methylpyrrole. The surface of the fibers is smooth on the scale of tens of nanometers, and there are no visible voids on this scale. Our results suggest that polypyrrole fiber growth can be controlled by varying the process parameters which govern the transport and flow pattern of the electrolyte across the electrode. The parameters in Table II have been found to reliably produce fibers 5–6 μm in diameter.

The parameters above (with the exception of the deposition solution and potential) were also ideal for the production of P3MT fibers with the same range of diameters. Scanning electron microscopy (SEM) results indicate that fibers are not subject to the formation of cracks or voids, even after several months in a storage container.

We have also shown that P3MT and PEDOT can be used to create a film coating over a 250 μm platinum wire in a standard three-electrode cell and that they share similar surface features when examined under SEM. The smoothness of these films is not as marked, and efforts are underway to improve this feature, as are preliminary studies of in vivo response to intracranial electrodes based on these films. The durability of the fibers and films, along with the aspect ratios obtained, make it likely that they will, indeed, be useful for in vivo measurements.

Experiments are presently underway to extend the fabrication method to other monomer/dopant combinations and to produce fibers with diameters on the order of 1 μm or less for monitoring neurotransmitter release in a rat model. Conducting polymer electrodes have been found to be particularly useful for detection of catecholamine-type neurotransmitters. There are a number of advantages of these electrodes. For example, they tend to show less tendency to be fouled by redox products or adsorbed biomolecules.[33,34] In many cases, these electrodes are capable of electrocatalysis of the oxidation of these neurotransmitters[3] and improving the reversibility of the redox couple.[35] These factors can lead to less incidence of interference from other molecules that traditionally interfere with analysis (such as ascorbate). Further, some instances have been found for a moderate degree of innate selectivity.[36,37]

Acknowledgments

The authors acknowledge the support of the National Science Foundation (DMR—521170) for the acquisition of the field-emission scanning electron microscope instrument employed in these studies.

Georgetown University assisted in meeting the publication costs of this article.

References

1. J. F. Rubinson and H. B. Mark, Jr., in *Conducting Polymers and Polymer Electrolytes*, pp. 2, Oxford University Press, New York (2003).
2. C. Allen, J. L. Peters, S. R. Sesack, and A. C. Michael, in *Monitoring Molecules in Neuroscience, Proceedings of the International Conference on In Vivo Methods*, 9th edition, Dublin, Ireland, June 16–19, pp. 89–90 (2001).
3. N. F. Atta, I. Marawi, K. L. Petticrew, H. Zimmer, H. B. Mark, and A. Galal, *J. Electroanal. Chem.*, **408**, 47 (1996).
4. X. Cui, V. A. Lee, Y. Raphael, J. A. Wiler, J. F. Hetke, D. J. Anderson, and D. C. Martin, *J. Biomed. Mater. Res.*, **56**, 261 (2001).
5. X. Cui, J. F. Hetke, J. A. Wiler, D. J. Anderson, and D. C. Martin, *Sens. Actuators, A*, **93**, 8 (2001).
6. J. H. Collier, J. P. Camp, T. W. Hudson, and C. E. Schmidt, *J. Biomed. Mater. Res.*, **50**, 574 (2000).
7. X. Cui, J. Wiler, M. Dzaman, R. A. Altschuler, and D. C. Martin, *Biomaterials*, **24**, 777 (2003).
8. S. A. Betchen, and M. Kaplitt, *Curr. Opin. Neurol.*, **16**, 487 (2003).

Downloaded on 2016-09-15 to IP 130.203.136.75 address. Redistribution subject to ECS terms of use (see ecsdl.org/site/terms_use) unless CC License in place (see abstract).

9. T. Loddenkemper, A. Pan, S. Neme, K. B. Baker, A. R. Rezai, D. S. Dinner, B. Erwin, J. Montgomery, and H. O. Lüders, *J. Clin. Neurophysiol.*, **18**, 514 (2001).
10. R. J. Christine Jérôme, *Angew. Chem., Int. Ed.*, **37**, 2488 (1998).
11. P. J. A. Kenis, R. F. Ismagilov, S. Takayama, G. M. Whitesides, S. Li, and H. S. White, *Acc. Chem. Res.*, **33**, 841 (2000).
12. H. Okuzaki and M. Ishihara, *Macromol. Rapid Commun.*, **24**, 261 (2003).
13. Y. Yang, J. Liu, and M. Wan, *Nanotechnology*, **13**, 770 (2002).
14. J. Huang, S. Virji, B. H. Weiller, and R. B. Kaner, *J. Am. Chem. Soc.*, **125**, 314 (2003).
15. J. Liu and M. Wan, *J. Mater. Chem.*, **11**, 404 (2001).
16. S. Li, C. W. Macosko, and H. S. White, *Science*, **259**, 957 (1993).
17. S. Li and H. S. White, *J. Electrochem. Soc.*, **140**, 2473 (1993).
18. H. X. He, C. Z. Li, and N. J. Tao, *Appl. Phys. Lett.*, **78**, 811 (2001).
19. D. H. Reneker and I. Chun, *Nanotechnology*, **7**, 216 (1996).
20. S. Li, C. Macosko, and H. White, *Science*, **259**, 957 (1993).
21. B. Meagher, D. Schwarcz, and M. Ohring, *J. Mater. Sci.*, **31**, 5479 (1996).
22. X. Cui and D. C. Martin, *Sens. Actuators B*, **89**, 92 (2003).
23. H. B. Mark, Jr, N. Atta, Y. L. Ma, K. L. Petticrew, H. Zimmer, Y. Shi, S. K. Lunsford, J. F. Rubinson, and A. Galal, *Bioelectrochem. Bioenerg.*, **38**, 229 (1995).
24. H. B. Mark, Jr, H. Zhang, S. K. Lunsford, O. Ceylan, A. I. Khaskelis, N. Atta, A. Galal, S. Hausner, J. F. Rubinson, G. C. Russell et al., *Anal. Chim. Acta*, **385**, 281 (1999).
25. H. Zhang, A. Galal, J. Rubinson, I. Marawi, T. Ridgway, S. Lunsford, H. Zimmer, and H. B. Mark, Jr, *Electrochim. Acta*, **23**, 3511 (1998).
26. H. Zhang, S. Lunsford, I. Marawi, J. Rubinson, and H. B. Mark, Jr, *J. Electroanal. Chem.*, **424**, 101 (1997).
27. H. Kato, O. Nishikawa, T. Matsui, S. Honma, and H. Kokado, *J. Phys. Chem.*, **95**, 6014 (1991).
28. A. J. Bard and L. R. Faulkner, in *Electrochemical Methods*, pp. 398–401, John Wiley & Sons, New York (2001).
29. M. Cai, M. D. Mowery, J. E. Pemberton, and C. E. Evans, *Appl. Spectrosc.*, **54**, 31 (2000).
30. F. Chen, G. Shi, J. Zhang, and M. Fu, *Thin Solid Films*, **424**, 283 (2003).
31. W. W. Chiu, J. Travas-Sejdic, R. P. Cooney, and G. A. Bowmaker, *Synth. Met.*, **155**, 80 (2005).
32. William W. Chiu, J. T. S. Cacute, and R. P. C. G. A. Bowmaker, *J. Raman Spectrosc.*, **37**, 1354 (2006).
33. N. F. Atta, G. C. Russell, Z. Wang, N. Akmal, J. F. Rubinson, S. K. Lunsford, E. Karagozler, O. Y. Ataman, H. Zimmer, H. B. Mark et al., *Turkish Journal of Chemistry*, **21**, 21 (1997).
34. J. Wang and R. Li, *Anal. Chem.*, **61**, 2809 (1989).
35. G. Erdogdu, H. B. Mark, and A. E. Karagozler, *Anal. Lett.*, **29**, 221 (1996).
36. H. Zhang, S. K. Lunsford, I. Marawi, J. F. Rubinson, and H. B. Mark, *J. Electroanal. Chem.*, **424**, 101 (1997).
37. A.-M. Yu, D.-M. Sun, and H.-Y. Chen, *Anal. Lett.*, **30**, 1643 (1997).

Downloaded on 2016-09-15 to IP 130.203.136.75 address. Redistribution subject to ECS terms of use (see ecsdl.org/site/terms_use) unless CC License in place (see abstract).